

# Study on Solidification of Chromium-Containing Sludge With Alkali Slag Combined With Attapulgite

**Huirong Lin**

Chongqing University

**Linghao Zeng**

Chongqing University

**Pengpeng Zhang**

Chongqing University

**Bingquan Jiao**

Chongqing University

**YanChyuan Shiau**

Chung Hua University

**Dongwei Li** (✉ [lironwei@cqu.edu.cn](mailto:lironwei@cqu.edu.cn))

Chongqing University

---

## Research Article

**Keywords:** sludge, heavy metal, attapulgite, alkaline activator, solidification/stabilization, geopolymer

**Posted Date:** May 11th, 2021

**DOI:** <https://doi.org/10.21203/rs.3.rs-465111/v1>

**License:** © ⓘ This work is licensed under a Creative Commons Attribution 4.0 International License. [Read Full License](#)

---

# Abstract

In order to solve the harm of hazardous waste chromium-containing sludge to humans and the environment, this paper uses attapulgite to strengthen alkali slag to prepare cementitious materials to solidify/stabilize chromium-containing sludge. Single-factor and orthogonal experiments were used to optimize the preparation parameters of alkali slag cementitious materials. The compressive strength, heavy metal leaching toxicity, and microscopic characterization of chromium-containing sludge solidified body were tested to investigate the solidification effect and mechanism of chromium-containing sludge. The results show that: The best content of attapulgite is 4%. The compressive strength of the solidified body decreased with the increase of chromium sludge content, and the leaching concentration of Cr and Cu increased with the rise of chromium-sludge content. The addition of attapulgite enhanced the compressive strength. Compared with the original chromium-containing sludge, the leaching concentration of heavy metals in the solidified body is significantly reduced. The XRD and FTIR analysis showed that the solidified body might solidify/stabilize heavy metals by physical encapsulation of amorphous form and chemical immobilization. This research realizes the use of waste to treat waste and provides the possibility for the application of solidified products in construction.

## 1 Introduction

Chromium-containing sludge is a hazardous waste discharged from industrial production, especially the chemical industry. It contains heavy metals such as chromium and lead, threatening ecological safety and human health(Yang et al. 2009). If the contaminated parts are not repaired, even if the chromium slag is properly treated, the environmental pollution caused by the chromium slag cannot be completely eliminated.

For the treatment of chromium-containing waste, there are mainly three types of methods: dry, wet and solidification methods(Fawcett 1984, Means et al. 1991, Vipulanandan &Krishnan 1990). The main content of the dry process is to mix heavy metal waste and reducing agent or adsorbents in a solid environment, and then convert the heavy metals into a more stable form. This method is too costly and may be ineffective for other heavy metal wastes. Mou et al(Mou et al. 2021) uses  $Fe_3O_4$  and  $C_6H_8O_7$  to reduce the chromium slag in a high-temperature environment, and the result proves that most of the chromium is converted to a residual state.

The wet method mainly uses a reducing agent to reduce chromium in a solution environment where chromium has been dissolved by acid and alkali. The advantage of wet detoxification is that the principle is simple and the detoxification is more thorough. However, this method consumes a large amount of reagents and has many procedures. Some scholars have studied the method of treating chromium slag with calcium sulfide in a reduced form, and found that the treatment efficiency of Cr(VI) is not complete(Graham et al. 2006, Wazne et al. 2007). Some scholars(Sekhar et al. 2003) have used microorganisms and plant components to detoxify heavy metal wastewater, and found that its effect is good and it is possible to replace the traditional sewage treatment technology. Solidification/stabilization (S/S) is a method of transforming a target substance into a stable state through complexation, precipitation, physical adsorption, ion exchange or electrostatic interaction. It has outstanding social, environmental and economic benefits(Wang et al. 2021a). Geopolymer is an innovative alkali-activated gelling material, which is an inorganic polymer with excellent properties produced by clay and aluminosilicate at normal temperature (Lee &Lee 2015, Xia et al. 2019). Compared with traditional

cement, geopolymer has better mechanical properties and corrosion resistance(Istuque et al. 2019). And through the mechanical properties and leaching level, the solidification efficiency can be analyzed intuitively(Zhang et al. 2016). Therefore, geopolymers are a popular choice for curing agents for the solidification/stabilization of heavy metals in recent years. The formation reaction process of geopolymers goes through the following steps: (1) mixing and dissolving of raw materials and alkali activator (2) Depolymerization and reorganization (3) Viscosity increase; (4) solidification and hardening; (5) crystallization, the gel continues to evolve towards crystallization(Juenger et al. 2011).

Gao et al.(Gao et al. 2014) has proved that in the preparation process of geopolymers, the  $\text{SiO}_2/\text{Na}_2\text{O}$  ratio of the reactants is obviously related to the properties of the product. The best value is 1.5. In the experiment of solidifying heavy metal slag, Zhang et al.(Zhang et al. 2020) demonstrated the influence of water content and alkalinity on the reaction rate and product strength, and the water content and alkalinity should be controlled within a reasonable range. It can be seen that the preparation of geopolymers is restricted by many conditions. Niu et al.(Niu et al. 2019) used bentonite-sulfoaluminate cement composite material to solidify chromium-containing hazardous waste, and found that it has a good solidification effect and compressive strength for heavy metals. Kim et al.(Kim et al. 2005) combined slag and calcium oxide to treat the sludge and found that its mechanical properties are good, and it can meet the capping requirements of landfills. Mao(Mao et al. 2019) uses bentonite as an additive to solidify lead-zinc smelting slag. Compared with using slag alone, its solidification effect and material properties are better. The effect of auxiliary additives is more obvious. This shows the prospect of using multiple raw materials to jointly prepare geopolymers.

Attapulgite (the mineral structure(Wang et al. 2018) is shown in the Fig. 1) is a kind of raw material rich in active silicon and aluminum components(Wang et al. 2018). It can form a dense and stable structure and absorb and solidify heavy metal ions under the condition of hydration and polymerization reactions. Attapulgite has a complex structure and its surface is rich in hydroxyl groups, which can be modified to enhance its own solidification effect on metals. Ren et al.(Ren et al. 2021) used attapulgite to treat the sludge and found that adding attapulgite can effectively promote the conversion of heavy metals into the residual state. It makes the heavy metals in the sludge less active. Liang, XF et al.(Liang et al. 2019) used modified attapulgite to treat cadmium-containing soil and found that the solidification effect was good. Xu, Congbin et al.(Xu et al. 2019) used modified attapulgite to solidify chromium-containing soil, and found that in addition to good solidification effect, the improved soil is more conducive to plant planting. Bhagat ed al.(Bhagat et al. 2021) used a data intelligence model to simulate the adsorption of lead by attapulgite, and found that the adsorption will change with the change of pH.

In this study, slag and attapulgite will be combined to prepare a solidified body to solidify chromium-containing sludge. It makes the solidified body have a certain strength, and can effectively improve the leaching level of heavy metals compared to the original. The mechanism will be analyzed by means of chemical characterization.

## **2 Experimental Materials, Instruments And Experimental Methods**

### **2.1 Main materials and their physical and chemical properties**

The attapulgite used in this experiment was provided by Changzhou Dingbang Mineral Products Technology Co., Ltd(China). The shape is white and yellowish powder, which has passed a 200-mesh sieve. Through X-ray fluorescence spectroscopy experimental analysis, the chemical composition of the attapulgite used was determined. The results are shown in Table 1. According to the above chemical composition, it can be seen that the main components of the attapulgite used in this experiment are SiO<sub>2</sub>, Al<sub>2</sub>O<sub>3</sub>, MgO, etc., and also contain a certain amount of Fe<sub>2</sub>O<sub>3</sub>, CaO and other substances that contain adsorptive properties. The XRD pattern (Fig. 2) shows that it contains crystal structure such as quartz, palygorskite (chain structure clay), dolomite, etc.

Table 1  
Chemical composition of attapulgite (wt.%)

SiO <sub>2</sub>	Al <sub>2</sub> O <sub>3</sub>	Fe <sub>2</sub> O <sub>3</sub>	MgO	CaO	K <sub>2</sub> O	TiO <sub>2</sub>	SO <sub>3</sub>	P <sub>2</sub> O <sub>5</sub>	Na <sub>2</sub> O	Other
55.26	12.52	10.06	8.55	8.02	2.15	1.62	0.78	0.43	0.20	0.41

Table 2  
The main chemical composition of chromium-containing sludge (wt.%)

PbO	Cr <sub>2</sub> O <sub>3</sub>	Fe <sub>2</sub> O <sub>3</sub>	CuO	NaO	Cl	SO <sub>3</sub>	SnO <sub>2</sub>	BaO	CaO	SiO <sub>2</sub>	NiO	Other
24.29	18.72	13.54	13.28	10.00	5.91	5.42	3.18	2.47	1.05	0.98	0.45	0.69

Table 3  
The main chemical composition of blast furnace slag(wt.%)

CaO	SiO <sub>2</sub>	Al <sub>2</sub> O <sub>3</sub>	MgO	S	TiO <sub>2</sub>	MnO	Fe <sub>2</sub> O <sub>3</sub>	K <sub>2</sub> O	Na <sub>2</sub> O	Others
40.85	29.69	15.91	7.23	2.33	1.40	0.87	0.71	0.44	0.26	0.31

Table 4  
Leaching of chromium-containing sludge(mg/L)

Cr	Cu	Pb
2022.53	3667.50	8.38

The object treated in this experiment is chromium-containing sludge was provided by Xinzhongtian Company(China). It contains heavy metals such as chromium and lead. Through X-ray fluorescence spectroscopy analysis, it can be known that its main chemical composition is shown in Tables 2. It can be seen from that chromium-containing sludge is rich in many types of heavy metals. Put the chromium-containing sludge into a drying box for drying, and determine the water content of the sludge for subsequent leaching toxicity experiments. The dried sludge is put into a roller ball mill for ball milling for 12 hours, the ball milled sludge is classified with a 200-mesh standard sieve, and the obtained sludge fine powder is used to prepare solidified body and leaching test. Several types of heavy metals can be leached by TCLP leaching (Table 4): Cr (2022.53mg/L), Cu (3667.5mg/L), Pb (8.38mg/L). Use X-ray diffraction pattern to analyze the phase structure of chromium-containing sludge, and get its XRD pattern, as shown in Fig. 3.

The blast furnace slag (BFS) used in the experiment is white powder and has passed a 200-mesh screen. Its chemical composition can be obtained by X-ray fluorescence spectroscopy, as shown in Table 3. The X-ray diffraction pattern of its mineral structure is shown in Fig. 4. Its mineral structure is dominated by gehlenite.

## 2.2 BFS based geopolymer production process

The slag and other active materials are dried in an oven and then taken out, and polished with a ball mill to pass a 200-mesh sieve. Prepare the alkaline activator that meets the requirements with water glass reagent and sodium hydroxide, and add a certain amount of water and then leave it for a period of time. Pour the active material and the alkali activator into a polyethylene beaker and stir well until the slurry state. After that, the adjusted slurry is filled into a mold with a size of 20mm×20mm×20mm. Place the mold on a vibrating table and vibrate to expel the air in it, and then compact it. Place the mold in a dry box with a set temperature for solidify for 7 days and measure its compressive strength. Take out the mold and place the solidified body in the maintenance room for a longer period of time for measurement.

## 2.3 Solidification/stabilisation of CCS

The sample with highest compressive strength (Obtained from single factor experiment and orthogonal experiment) was selected for solidification of CSS. The different proportions (10%, 20%, 30%, 40%, 60%, 70% and 80%) of CSS were solidified in composite based geopolymer after drying at 105°C for 6 h.

## 2.4 Compressive strength measurement

The determination of compressive strength complies with the standard of GB/T17671-1999. All tests were performed using a compressive strength multifunctional testing machine (AGN-250, Shimadzu, Japan), and the test results were averaged.

## 2.5 Analysis and test methods

(1) The compressive strength test is to determine the geopolymer and solidified body according to GB/T17671-1999 "Cement Mortar Strength Test Method (ISO Method)".

(2) The leaching experiment refers to the US EPA standard, adopts the TCLP method (Toxicity Characteristic Leaching Procedure, TCLP) to leach the original sludge and the solidified sludge, and refers to its leaching concentration standard.

Solidification efficiency of heavy metals was determined by the following formulas:

$$W=1-M1/M2$$

The "W" represents the solidification efficiency of heavy metals. "M1" represents the leaching concentration of the solidified body, and "M2" represents the leaching concentration of the sludge.

(3) The determination of total chromium in the leachate of sludge and solidified body is carried out in accordance with the standard HJ 749–2015 "Determination of Total Chromium in Solid Wastes by Flame Atomic Absorption Spectrophotometry".

(4) Characterization analysis

The crystal composition before and after solidification/stabilization was observed by XRD (PANalytical B. V., Holland) under the following conditions: CuK $\alpha$  radiation, 40kV, 30mA. The molecular structure was analyzed

by FTIR spectroscopy (Thermo Nicolet-5700 Corporation, USA).

## 3 Result And Discussion

### 3.1 single-factor experiment

With reference to Huang's research(Huang et al. 2015), the liquid-solid ratio of alkali activator (water glass) content and the modulus of alkali activator have a great influence on the preparation reaction. Set up single-factor experiments based on several types of indicators. The solidify temperature is 25°C. The compressive strength was measured after 7 days of solidify. The single-factor experiment ratio is shown in Table 5.

The experimental results of the influence of the liquid-solid ratio in the single-factor experiment are shown in Fig. 5. It can be obtained when the content of the alkali activator is 10% and the modulus of the alkali activator is 1.5. The compressive strength of the gel reaches the maximum when the liquid-to-solid ratio is about 0.24. The liquid-to-solid ratio affects the fluidity, concentration and stirring(Yahya et al. 2015) of the reactants, and should not be too small. But it can't be lower, otherwise the cavity and the dilution effect(Barbosa et al. 2000) will affect the intensity.

The results of the single factor experiment on the influence of the dosage of the alkaline activator are shown in Fig. 5. It can be obtained when the liquid-solid ratio is 0.27 and the modulus of the alkali activator is 1.5. The compressive strength of the gel reaches the maximum when the content of the alkali activator is about 13%. In addition to the stimulating effect, the alkaline activator also provides the reactant. However, too much stimulant will destroy the proper silicon-to-aluminum ratio, and will cover the surface of the reactant to prevent the reaction from proceeding(Alonso &Palomo 2001, Somna et al. 2011).

Table 5  
Single factor experiment ratio

Num	Liquid-solid ratio	Alkaline activator dosage(%)	Alkaline activator modulus
1	0.21	10	1.5
2	0.24	10	1.5
3	0.27	10	1.5
4	0.30	10	1.5
5	0.27	7	1.5
6	0.27	10	1.5
7	0.27	13	1.5
8	0.27	16	1.5
9	0.27	10	0.9
10	0.27	10	1.2
11	0.27	10	1.8

## 3.2 Orthogonal experiment

Set appropriate parameters according to the results of single factor experiment, and carry out orthogonal experiment. In this section of the experiment, "liquid-solid ratio", "alkali activator dosage", and "alkali activator modulus" are orthogonal factors, and each factor is set to 3 levels. Design three-factor and three-level orthogonal experiments to analyze its relationship with the properties of geopolymer materials and determine the best combination parameters of each raw material. The factor level table is shown in Table 6. According to the principle of orthogonal experiment, the calculation method of design orthogonal experiment table range analysis and results is shown in Table 7.

Table 6  
Orthogonal three-factor three-level table

Level/factor	Alkaline activator dosage(%)	Alkaline activator modulus	Liquid-solid ratio
1	11	1.3	0.22
2	13	1.5	0.24
3	15	1.7	0.26

Table 7  
Orthogonal Design Table

Experiment number	Alkaline activator dosage	Alkaline activator modulus	Liquid-solid ratio	$Y_i$ (Compressive strength)
1	1	1	1	73.28
2	1	2	2	80.79
3	1	3	3	91.56
4	2	1	2	82.72
5	2	2	3	89.53
6	2	3	1	95.47
7	3	1	3	78.51
8	3	2	1	79.51
9	3	3	2	77.93
$K_{j1}$	$y_1 + y_2 + y_3$	$y_1 + y_4 + y_7$	$y_1 + y_6 + y_8$	
$K_{j2}$	$y_4 + y_5 + y_6$	$y_2 + y_5 + y_8$	$y_2 + y_4 + y_9$	
$K_{j3}$	$y_7 + y_8 + y_9$	$y_3 + y_6 + y_9$	$y_3 + y_5 + y_7$	
$k_{j1}$	$K_{11}/m = 81.88$	$K_{21}/m = 78.17$	$K_{31}/m = 82.75$	
$k_{j2}$	$K_{12}/m = 89.24$	$K_{22}/m = 83.28$	$K_{32}/m = 80.48$	
$k_{j3}$	$K_{13}/m = 78.65$	$K_{23}/m = 88.32$	$K_{33}/m = 86.53$	
R	$\max\{k_{1i}\}-\min\{k_{1i}\}$ =10.59	$\max\{k_{2i}\}-\min\{k_{2i}\}$ =10.15	$\max\{k_{3i}\}-\min\{k_{3i}\}$ =18.16	
Optimal	$A_2$	$B_3$	$C_3$	

According to the results of the orthogonal experiment, the best experiment ratio is 13% of the alkali activator, the modulus of the alkali activator is 1.7, and the liquid-solid ratio is 0.26. It can be seen from the extreme contrast that the relative importance of the three factors (alkali activator content, alkali activator modulus, liquid-solid ratio) that affect the compressive strength of the gel is different. Among them, the liquid-solid ratio has the greatest influence, and the influence of the dosage of the alkali activator and the modulus of the alkali activator is relatively small.

In summary, the best ratio of pure slag preparation gelled body obtained by orthogonal experiment is: the content of alkali activator is 13%, the modulus of alkali activator is 1.7, and the liquid-solid ratio is 0.26. It was verified by experiments that the compressive strength of the gel under this condition (solidify time : 7 days) reached 96.07 MPa.

### 3.3 The influence of attapulgit content

According to the experimental results (Fig. 6), when the addition amount of attapulgite is small, the reason for the increase in strength should be that the particle size of attapulgite and slag are different, and mutual filling makes the overall structure more compact and stable. When the content of attapulgite gradually increased more than 6.5%, the strength began to decrease significantly. This may be because an excessive amount of attapulgite reduces the intensity of the hydration reaction. According to experiments, the content of attapulgite is determined to be 4%. Although the strength is not improved compared with the gel without attapulgite, it still maintains a high level.

### **3.4 Compressive strength of solidified soil**

It can be seen from the results (Fig. 7) that with the incorporation of chromium-containing sludge, the strength of the gel decreases significantly. From 10–80%, the strength gradually decreases. Through analysis, the active components in chromium-containing sludge, such as silicon-aluminum salt and active binding components, are far lower than the related components contained in the slag, which also reduces the strength of the hydration reaction. In addition, the sulfur and chlorine in chromium-containing sludge and other materials may affect the stable structure of the gel; the heavy metal components in the sludge also affect the progress of the hydration reaction, which may be due to the low solubility of some heavy metal compounds. And its participation in the reaction is relatively small, making the hydration reaction not as smooth as before. In addition, some researchers (Chi 2004) believe that the water absorption rate may affect the strength of the solidified body. The water absorption rate of chromium-containing sludge is significantly lower than that of slag, which reduces the cementitious components produced in the mixture and ultimately reduces the compressive strength. According to the "Concrete Strength Inspection and Evaluation Standard" (GB/T 50107 – 2010), the minimum strength standard C7.5 has a strength of 10.8MPa. When the sludge blending amount exceeds 30%, its strength is already lower than 10MPa, and the strength of 20% blending amount is still close to the strength requirement of C7.5 in the "Concrete Strength Inspection and Evaluation Standard". According to the US EPA standard (landfill strength requirement  $\geq 0.35$ MPa), the compressive strength of the solidified body is required for landfill. The compressive strength test was carried out after solidify for 7 days, and the results are shown in Figure. According to the "Concrete Strength Inspection and Evaluation Standard" (GB/T 50107 – 2010), the minimum strength standard C7.5 has a strength of 10.8 MPa. According to the experimental results, regardless of the addition of attapulgite, the amount of chromium-containing sludge in the solidified body should not exceed 20%, but the addition of attapulgite can greatly improve its mechanical properties. This is because the raw material is mainly blast furnace slag. The added attapulgite can not only serve as fine aggregates to fill the internal defects of the solidified body, but also because the attapulgite adsorbs some heavy metals, the content of heavy metals that hinder the hydration reaction can be reduced. Attapulgite promotes the hydration reaction due to the stabilization of heavy metal ions (Wang et al. 2021b), which enhances the compressive strength of the solidified body.

### **3.5 The leaching concentration of the solidified body**

Table 8  
List of leaching concentrations

CCS content	Cr (mg/L)		Cu (mg/L)		Pb (mg/L)	
	×	√	×	√	×	√
Add attapulgite or not	×	√	×	√	×	√
10%	102.60	52.10	0	20.16	146.50	14.40
20%	120.40	92.73	18.60	67.77	59.40	1.00
30%	130.00	100.20	54.00	112.86	6.50	0
40%	140.60	130.50	123.20	181.26	4.70	0
50%	163.50	161.46	211.40	235.71	2.10	0
60%	207.20	211.14	297.40	333.36	0	0
70%	254.20	223.38	351.30	423.81	0	0
80%	346.70	267.84	422.90	538.02	0	0

Table 9  
The solidify efficiency of heavy metals in different content after adding attapulgite

Dosage/ solidify efficiency (%)	10%	20%	30%	40%	50%	60%	70%	80%
Cr	90.64	91.67	94.00	94.14	94.20	93.68	94.27	93.98
Cu	96.20	93.61	92.91	91.45	91.11	89.52	88.58	87.32
Pb	98.57	99.95	100	100	100	100	100	100

According to HJ/T 300–2007 "Solid Waste-Leaching Toxicity Leaching Method-Acetic Acid Buffer Solution Method", the solidified body after 28 days of solidify time is subjected to leaching test, and then the solidification effect of heavy metals is comprehensively investigated. The leaching of Cr, Cu, Pb is shown in Table 8 and Fig. 8.

The leaching level of Cr can be seen from the Fig. 8 above. After the 28-day solidify time is over, the chromium leaching level increases as the sludge content increases. After 28 days of solidify, the internal reaction of the solidified soil proceeded sufficiently to form a stable polymer structure(Barbosa et al. 2000). This structure strengthens the restraint on heavy metals. The leaching concentration of the composite solidified body with attapulgite added is generally lower than that of the pure slag solidified body without adding attapulgite. In addition, when the content of chromium-containing sludge increases, the compressive strength of the solidified body decreases. The compressive strength shows the compactness and stability of the solidified body itself. The higher the compressive strength, the better the ability to solidify heavy metals. When the content of chromium-containing sludge reaches 60%, the leaching level of chromium after adding attapulgite is relatively close to the leaching level without adding attapulgite. It may be because at this dosage, the amount of slag in the solidified body is not large and cannot maintain a certain strength, and the dosage of attapulgite is also small and cannot absorb more chromium. However, as the content of chromium-containing sludge continues to increase, the strength decreases, and the chromium in the solidified body is more likely to enter the leachate, and then be absorbed by the more effective attapulgite in the liquid(Ma et al. 2021). It can

be seen that by adding attapulgite, the compressive strength of the solidified body can be increased, and the leaching concentration can be reduced accordingly.

Figure 8 shows the comparison between the leaching of copper after adding attapulgite and the case without adding attapulgite. It can be seen from the figure that the solidified body after adding attapulgite does not help the absorption of  $\text{Cu}^{2+}$ . The reason may be that the addition of attapulgite is not conducive to the development of strength compared with pure slag. When the mixing amount of chromium-containing sludge gradually increases and exceeds the adsorption/solidification limit of the composite solidified body, compared with the solidified body prepared from pure slag, the solidified body with attapulgite is not as stable as pure slag because of the mineral structure. Therefore, the effect of solidify of the silicon-aluminum polymer structure is relatively less obvious. In addition, the selective adsorption characteristics and adsorption balance of attapulgite clay minerals have led to different adsorption/solidification effects on different heavy metals(He et al. 1999), and the adsorption capacity of unmodified attapulgite for Cu should not be as good as that of the others. So there is a reason why the leaching concentration of copper is increased when the amount of doping increases in the later period. In an environment where both  $\text{Pb}^{2+}$  and  $\text{Cu}^{2+}$  exist, the  $\text{Cu}^{2+}$  absorption sites of attapulgite will be preempted by Pb(Xu et al. 2021). A further explanation comes from the study of Du et al.(Du et al. 2016). They believe that  $\text{Pb}^{2+}$  is preferentially adsorbed on attapulgite over  $\text{Cu}^{2+}$  and occupies the adsorption sites on the amino group, which inhibits the adsorption of  $\text{Cu}^{2+}$ .

From Fig. 8, it can be seen that the leaching concentration of Pb has a different trend from that of Cr and Cu. As the content of chromium-containing sludge increases, the leaching concentration of Pb gradually decreases, until the content reaches 50% and there is almost no leaching. It can be seen that the leaching effect of Pb in an acidic environment is different than other heavy metal ions. Studies(Muhammad et al. 2018) pointed out that the leaching level of  $\text{Pb}^{2+}$  in an aggressive environment (such as acid) will drop sharply because it is in an amorphous environment, and the chemical reaction relationship at this time hinders the performance of leaching. Luo Zejiao(Luo et al. 2014) also found through experiments that the leaching of Pb is very insignificant in a near neutral environment, and after adding an alkaline leaching agent represented by NaOH, the leaching of Pb begins to increase significantly. The research of Chen Haojing(Chen 2008) supports this view. He conducted fly ash leaching experiments and found that the leaching ratio of Pb in a pH greater than 3 to neutral environment is basically 0. It can be explained that in this experiment, the solidified target chromium-containing sludge is acidic, and with the addition of alkaline slag (the amount of chromium-containing sludge is reduced), (gelled body/solidified body) acidic corrosive medium environment began to change, and the leaching of Pb also manifests itself. In addition, it can be seen that before and after adding attapulgite, the leaching concentration of lead during the leaching process of the solidified body decreases as the dose increases. This also verifies that the appearance of alkali slag breaks the original acidic medium leaching environment and makes the leaching effect more obvious. Although the trend is the same, the composite solidified body added with attapulgite shows a better solidification effect. Compared with before adding attapulgite, the leaching concentration of Pb after adding attapulgite is greatly reduced, the largest decrease is more than 90%, and the undetected content appears earlier(It reaching 30%). The leaching concentration of lead in the solidified body prepared from pure slag does not reach zero until the content reaches 60%. It shows that after adding attapulgite, the solidify effect of the solidified body on Pb is obviously improved.

Through comparison, it can be found that attapulgite can reduce the leaching concentration of heavy metals such as Cr and Pb within a certain range. Attapulgite has significant adsorption/solidification effects on several types of heavy metals. From Table 9, it can be seen that the solidification efficiency of the solidified body after adding attapulgite is maintained at a relatively high level. The adsorption effect of attapulgite on Cu is not ideal. This can be used to modify the attapulgite in subsequent experiments to improve its adsorption capacity, so that it can effectively adsorb  $\text{Cu}^{2+}$  in the presence of  $\text{Pb}^{2+}$ .

### 3.6 XRD analysis

It can be seen from the XRD pattern (Fig. 9) that the structure of the gelatinous mineral prepared by the alkali-excited slag is mainly calcium aluminum yellow feldspar, CSH gel (free calcium oxide and calcium sulfate in the blast furnace slag and the silicon-aluminum component reacted under the action of the alkaline activator to form hydrated calcium silicate and aluminum), the whole is an amorphous product. According to research (Puertas et al. 2005, Liu et al. 2017), when the ratio of  $\text{SiO}_2/\text{Al}_2\text{O}_3$  is lower than 4.5 (this experiment uses the main raw material slag, the ratio is lower than 4.4, and the content of attapulgite is extremely small) hydration product is CSH Gel Mainly. After mixing the sludge, the peak intensity of the yellow feldspar decreases, indicating that the amorphous heavy metal components should be embedded in the gel solidification body. After the addition of attapulgite, more diffraction peaks of heavy metal salts appeared, indicating that heavy metals were bound by the C-S-H gel and transformed into a class of amorphous substances. The above action causes the heavy metal components to be solidified. After adding attapulgite, the XRD pattern did not change too much, which may be due to the low content of attapulgite (4%). In addition, no more obvious characteristic peaks appeared after adding attapulgite, indicating that the addition of attapulgite did not change the product of the cementing material, and it was only used as an adsorbent for heavy metal ions and as an aggregate in the slurry to improve the performance of the cementing material.

### 3.7 FTIR analysis

Perform FTIR test on pure gel and solidified body, and analyze the results.

According to the analysis of FTIR results (Fig. 10), whether it is made of pure gel or solidified body mixed with chromium-containing sludge, several samples have relatively wide vibration bands near the wave numbers of  $3350\text{cm}^{-1}$  and  $1640\text{cm}^{-1}$ . These two places correspond to tensile vibration and bending vibration of H-O-H respectively, indicating that bound water is formed after the completion of the hydration reaction (Bernal et al. 2011). There are many weak absorption peaks near  $3500\text{cm}^{-1}$ - $4000\text{cm}^{-1}$  in the wavenumber, which should be the stretching vibration of the hydroxyl group in the hydrated aluminum compound (Navarro et al. 2010). The peak near the  $1412\text{cm}^{-1}$  wavenumber is the bending vibration of O-C-O, which has a certain relationship with the reaction of alkali metal oxides with  $\text{CO}_2$  (Andini et al. 2008, Yousuf et al. 1993). In the FTIR results of the pure slag gelatinous body, an absorption peak appeared at around  $935\text{cm}^{-1}$  wavenumber and was significantly weakened in the solidified body, and an absorption peak appeared at  $861\text{cm}^{-1}$  wavenumber (Si-O bending vibration) in the solidified body, which may be due to The Si-OT (T: Si or Al) stretching vibration produced by the tetrahedron of CSH, it indicates that the hydration reaction produces CSH gel (Kovtun et al. 2015). The wave number range of about  $421\text{cm}^{-1}$  is caused by the bending vibration of the Si-O-Si and O-Si-O bonds. The right shift or weakening of absorption peaks such as Si-O-T stretching vibration, Si-O-Si and Al-O-Si symmetric stretching vibration should be attributed to the substitution of heavy metals for Si in the CSH

structure or the influence of heavy metals on the degree of polymerization of CSH, it Changed the binding environment of the gel(Bakharev et al. 2003). After adding attapulgite soil, H-O-H tensile vibration appeared near the wave number of  $3350\text{ cm}^{-1}$ , and bending vibration of H-O-H appeared near the wave number of  $1640\text{ cm}^{-1}$ . The wave number and peak value did not change significantly, indicating that the generation of bound water was not affected. At the same time, it can be observed that after the addition of attapulgite, the wave number of the main peaks before and after the solidification of heavy metals decreases and the band shift phenomenon becomes smaller. This may be due to the ionization of the attapulgite with heavy metal ions after the addition of attapulgite. The exchange effect produces a change in vibration energy(Mao et al. 2019). The change of the peak value of each wave is also affected by the guarantee of the hydration degree of the cementitious material after the excellent adsorption performance of attapulgite for heavy metals. The silicon-aluminum-oxygen in the reaction product is single negatively charged, which plays a role in balancing the charge and stably bonding the heavy metal ions in the gel. In addition, compared with the case where attapulgite is not added, the FTIR results of the solidified body of attapulgite show that there are more faint and disordered peaks from  $420\text{cm}^{-1}$  to  $680\text{cm}^{-1}$ . This shows the vibration of the free silica of Si-O-Si(Zhang et al. 2021), and its band shifts to the left, showing that the more active free silica gradually decomposes and participates in the solidify process.

## 4 Conclusion

In this study, blast furnace slag and attapulgite was used as the main raw material, and sodium silicate reagent was used as the alkali activator to prepare alkali slag cementitious material, which was used to solidify chromium-containing sludge. The study analyzed the physical and chemical properties of raw materials, optimized the preparation parameters of alkali slag cementitious materials through single factor experiment and orthogonal experiment, and studied the stability of chromium-containing sludge solidified body. This paper analyzes the physical and chemical properties of chromium-containing sludge through XRD, FTIR, TCLP leaching and other analytical testing methods, and explores the solidification mechanism of alkali slag cementitious materials on chromium-containing sludge. The following main conclusions are obtained:

☒The preparation parameters of alkali slag cementitious materials are optimized through single factor experiment and orthogonal experiment. The optimal combination of parameters is: liquid-solid ratio 0.26, water glass modulus 1.7, and alkali activator content 13%. In the experiment with the addition amount of attapulgite as a single factor, it can be seen that the addition amount of 4% attapulgite in the range of a small amount of addition is the highest amount of compressive strength results, which is 71.35MPa.

☒Use chromium-containing sludge to partially replace blast furnace slag to prepare chromium-containing sludge solidification body, which realizes the solidification/stabilization of chromium-containing sludge by alkali slag cementing materials. The compressive strength test shows that the chromium-containing sludge solidified body has good mechanical properties (compressive strength > 10MPa at a content of 20% chromium-containing sludge). It has the prospect of building materials application and can meet the requirements of landfill strength. The results of heavy metal leaching experiments show that the leaching performance of heavy metals in the solidified body has decreased significantly compared with the original chromium-containing sludge. After adding attapulgite, the compressive strength of the solidified body of chromium-containing sludge with the same content has been significantly improved, and the leaching

performance has also been significantly improved. The leaching concentration of heavy metals such as chromium and lead decreased. It shows that the incorporation of attapulgite improves the solidification/stabilization effect of alkali slag cementitious materials on chromium-containing sludge.

Analysis of XRD, FTIR and other results showed that the reaction products of alkali slag cementitious material and solidified chromium-containing sludge mostly exist in amorphous form, and the heavy metals in chromium-containing sludge may participate in complex chemical reactions. It causes the band shift in FTIR. This change becomes smaller after adding attapulgite. The solidification mechanism of alkali slag cementitious material plus attapulgite to chromium-containing sludge is mainly physical encapsulation and chemical fixation. The addition of attapulgite promotes the hydration reaction in the solidified body when the chromium-containing sludge is added. It improves the mechanical properties of the solidified material through pore filling and its own adsorption/solidification of heavy metals, which also improves the solidification/stabilization effect on heavy metals.

## Declarations

### Ethical Approval

Not applicable

### Consent to Participate

Yes

### Consent to Publish

Yes

### Authors Contributions

Huirong Lin: Investigation; Methodology; Formal analysis; Roles/Writing - original draft

Linhao Zeng: Software; Writing - review & editing

Pengpeng Zhang: Methodology; Formal analysis; Validation

Binquan Jiao: Supervision; Conceptualization; Validation

YanChyuan Shiau: Visualization; Resources

Dongwei Li: Supervision; Conceptualization

### Availability of data and materials

All data generated or analysed during this study are included in this published article. And all data are fully available without restriction.

## Funding

No

## Conflicts of interest

There are no conflicts to declare.

## Acknowledgments

No

## References

1. Alonso S, Palomo A (2001) Alkaline activation of metakaolin and calcium hydroxide mixtures: influence of temperature, activator concentration and solids ratio. *Mater Lett* 47:55–62
2. Andini S, Cioffi R, Colangelo F, Grieco T, Montagnaro F, Santoro L (2008) Coal fly ash as raw material for the manufacture of geopolymer-based products. *Waste Manage* 28:416–423
3. Bakharev T, Sanjayan JG, Cheng YB (2003) Resistance of alkali-activated slag concrete to acid attack. *Cement Concrete Res* 33:1607–1611
4. Barbosa VFF, MacKenzie KJD, Thaumaturgo C (2000) Synthesis and characterisation of materials based on inorganic polymers of alumina and silica: sodium polysialate polymers. *Int J Inorg Mater* 2:309–317
5. Bernal SA, Provis JL, Rose V, de Gutierrez RM (2011) Evolution of binder structure in sodium silicate-activated slag-metakaolin blends. *Cement Concrete Comp* 33:46–54
6. Bhagat SK, Paramasivan M, Al-Mukhtar M, Tiyasha T, Pyrgaki K, Tung TM, Yaseen ZM (2021) Prediction of lead (Pb) adsorption on attapulgite clay using the feasibility of data intelligence models. *Environ Sci Pollut Res Int*
7. Chen HQ (2008) Leaching Behavior of Zn, Pb and Cu from MSWI Fly Ash. *Journal of Technology* 8:307–310
8. Chi DH (2004) The Study on the Solidification/Stabilization of Municipal Solid Waste incinerator fly ash in cement mortars. Master Thesis, Donghua University
9. Du H, Chen W, Cai P, Rong X, Feng X, Huang Q (2016) Competitive adsorption of Pb and Cd on bacteria-montmorillonite composite. *Environ Pollut* 218:168–175
10. Fawcett HW (1984) Toxic and Hazardous Waste-Disposal. *Prof Saf* 29 2:42–42 Options for Stabilization Solidification - Pojasek,Rb.
11. Gao K, Lin K-L, Wang D, Hwang C-L, Shiu H-S, Chang Y-M, Cheng T-W (2014) Effects SiO<sub>2</sub>/Na<sub>2</sub>O molar ratio on mechanical properties and the microstructure of nano-SiO<sub>2</sub> metakaolin-based geopolymers. *Constr Build Mater* 53:503–510
12. Graham MC, Farmer JG, Anderson P, Paterson E, Hillier S, Lumsdon DG, Bewley RJF (2006) Calcium polysulfide remediation of hexavalent chromium contamination from chromite ore processing residue. *Sci Total Environ* 364:32–44

13. He HP, Guo LH, Xie XD, Peng JL (1999) Experimental studies on the selective adsorption of  $\text{Cu}^{2+}$ ,  $\text{Pb}^{2+}$ ,  $\text{Zn}^{2+}$ ,  $\text{Cd}^{2+}$ ,  $\text{Cr}^{3+}$  ions on Montmorillonite, Illite and Kaolinite and the influence of medium conditions *Acta Mineralogica Sinica*. 231–235
14. Huang Yu, Li S, Li L (2015) Preparation and properties of geopolymer from blast furnace slag %J *Materials Research Innovations*. 19
15. Istuque DB, Soriano L, Akasaki JL, Melges JLP, Borrachero MV, Monzo J, Paya J, Tashima MM (2019) Effect of sewage sludge ash on mechanical and microstructural properties of geopolymers based on metakaolin. *Constr Build Mater* 203:95–103
16. Juenger MCG, Winnefeld F, Provis JL, Ideker JH (2011) Advances in alternative cementitious binders. *Cement Concrete Res* 41:1232–1243
17. Kim EH, Cho JK, Yim S (2005) Digested sewage sludge solidification by converter slag for landfill cover. *Chemosphere* 59, 387 – 95
18. Kovtun M, Kearsley EP, Shekhovtsova J (2015) Chemical acceleration of a neutral granulated blast-furnace slag activated by sodium carbonate. *Cement Concrete Res* 72:1–9
19. Lee NK, Lee HK (2015) Reactivity and reaction products of alkali-activated, fly ash/slag paste. *Constr Build Mater* 81:303–312
20. Liang XF, Li N, He LZ, Xu YM, Huang QQ, Xie ZL, Yang F (2019) Inhibition of Cd accumulation in winter wheat (*Triticum aestivum* L.) grown in alkaline soil using mercapto-modified attapulgite. *Sci Total Environ* 688:818–826
21. Liu Z, Zhou Y, Kong FL, Sun ZM, Qu MX (2017) Microstructure and Properties of Alkali-activated Blast Furnace Slag Based Geopolymer *Bulletin of the Chinese Ceramic Society*. 36, 1830–1834
22. Luo ZJ, Liu P, Jia N (2014) Leaching Toxicity Method of Lead Extraction from Soil Environmental. *Science Technology* 37:86–89
23. Ma H, Zhang XF, Wang ZG, Song L, Yao JF (2021) Flexible cellulose foams with a high loading of attapulgite nanorods for  $\text{Cu}^{2+}$  ions removal. *Colloid Surface A* 612
24. Mao YH, Muhammad F, Yu L, Xia M, Huang X, Jiao BQ, Shiao YC, Li DW (2019) The Solidification of Lead-Zinc Smelting Slag through Bentonite Supported Alkali-Activated Slag Cementitious Material. *Int J Env Res Pub He* 16
25. Means J, Heath J, Barth E, Monlux K, Solare J (1991) The Feasibility of Recycling Spent Hazardous Sandblasting Grit into Asphalt Concrete, *Waste Materials in Construction*. *Studies in Environmental Science*, pp 553–560
26. Mou HY, Liu WC, Zhao LL, Chen WQ, Ao TQ (2021) Stabilization of hexavalent chromium with pretreatment and high temperature sintering in highly contaminated soil. *Front Env Sci Eng* 15
27. Muhammad F, Huang X, Li S, Xia M, Zhang ML, Liu Q, Hassan MAS, Jiao BQ, Yu L, Li DW (2018) Strength evaluation by using polycarboxylate superplasticizer and solidification efficiency of  $\text{Cr}^{6+}$ ,  $\text{Pb}^{2+}$  and  $\text{Cd}^{2+}$  in composite based geopolymer. *J Clean Prod* 188:807–815
28. Navarro C, Diaz M, Villa-Garcia MA (2010) Physico-Chemical Characterization of Steel Slag. Study of its Behavior under Simulated Environmental Conditions. *Environ Sci Technol* 44:5383–5388

29. Niu MD, Li GX, Wang Y, Cao L, Han LL, Li QQ, Song ZP (2019) Immobilization of Pb<sup>2+</sup> and Cr<sup>3+</sup> using bentonite-sulfoaluminate cement composites. *Constr Build Mater* 225:868–878
30. Puertas F, Palacios M, Vázquez T (2005) Carbonation process of alkali-activated slag mortars. *Journal of Materials Science* 41:3071–3082
31. Ren J, Dai L, Tao L (2021) Stabilization of heavy metals in sewage sludge by attapulgite. *J Air Waste Manage* 71:392–399
32. Sekhar KC, Kamala CT, Chary NS, Anjaneyulu Y (2003) Removal of heavy metals using a plant biomass with reference to environmental control. *Int J Miner Process* 68:37–45
33. Somna K, Jaturapitakkul C, Kajitvichyanukul P, Chindaprasirt P (2011) NaOH-activated ground fly ash geopolymer cured at ambient temperature. *Fuel* 90:2118–2124
34. Vipulanandan C, Krishnan S (1990) Solidification Stabilization of Phenolic Waste with Cementitious and Polymeric Materials. *J Hazard Mater* 24:123–136
35. Wang L, Rinklebe J, Tack FMG, Hou D (2021a) A review of green remediation strategies for heavy metal contaminated soil. *Soil Use and Management*
36. Wang Q, Wen J, Hu X, Xing L, Yan C (2021b) Immobilization of Cr(VI) contaminated soil using green-tea impregnated attapulgite. *J Clean Prod* 278
37. Wang Y, Feng Y, Jiang J, Yao J (2018) Designing of Recyclable Attapulgite for Wastewater Treatments: A Review. *ACS Sustainable Chemistry Engineering* 7:1855–1869
38. Wazne M, Jappilla AC, Moon DH, Jagupilla SC, Christodoulatos C, Kim MG (2007) Assessment of calcium polysulfide for the remediation of hexavalent chromium in chromite ore processing residue (COPR). *J Hazard Mater* 143:620–628
39. Xia M, Muhammad F, Zeng LH, Li S, Huang X, Jiao BQ, Shiao Y, Li DW (2019) Solidification/stabilization of lead-zinc smelting slag in composite based geopolymer. *J Clean Prod* 209:1206–1215
40. Xu CB, Qi J, Yang WJ, Chen Y, Yang C, He YL, Wang J, Lin AJ (2019) Immobilization of heavy metals in vegetable-growing soils using nano zero-valent iron modified attapulgite clay. *Sci Total Environ* 686:476–483
41. Xu L, Liu YN, Wang JG, Tang Y, Zhang Z (2021) Selective adsorption of Pb<sup>2+</sup> and Cu<sup>2+</sup> on amino-modified attapulgite: Kinetic, thermal dynamic and DFT studies. *J Hazard Mater* 404
42. Yahya Z, Abdullah MMA, Hussin K, Ismail KN, Abd Razak R, Sandu AV (2015) Effect of Solids-To-Liquids, Na<sub>2</sub>SiO<sub>3</sub>-To-NaOH and Curing Temperature on the Palm Oil Boiler Ash (Si plus Ca) Geopolymerisation System. *Materials* 8:2227–2242
43. Yang J, Chai LY, Wang YY, He XW (2009) Transportation and distribution of chromium in the anaerobic sludge treating the chromium-containing wastewater. *Int J Environ Pollut* 38:256–266
44. Yousuf M, Mollah A, Hess TR, Tsai YN, Cocke DL (1993) An Ftir and Xps Investigations of the Effects of Carbonation on the Solidification Stabilization of Cement-Based Systems-Portland Type-V with Zinc. *Cement Concrete Res* 23:773–784
45. Zhang P, Muhammad F, Yu L, Xia M, Lin H, Huang X, Jiao B, Shiao Y, Li D (2020) Self-cementation solidification of heavy metals in lead-zinc smelting slag through alkali-activated materials. *Constr Build Mater* 249

46. Zhang WY, Qian LB, Chen Y, Ouyang D, Han L, Shang X, Li J, Gu MY, Chen MF (2021) Nanoscale zero-valent iron supported by attapulgite produced at different acid modification: Synthesis mechanism and the role of silicon on Cr(VI) removal. *Chemosphere* 267
47. Zhang ZK, Li AM, Wang XX, Zhang L (2016) Stabilization/solidification of municipal solid waste incineration fly ash via co-sintering with waste-derived vitrified amorphous slag. *Waste Manage* 56:238–245

## Figures

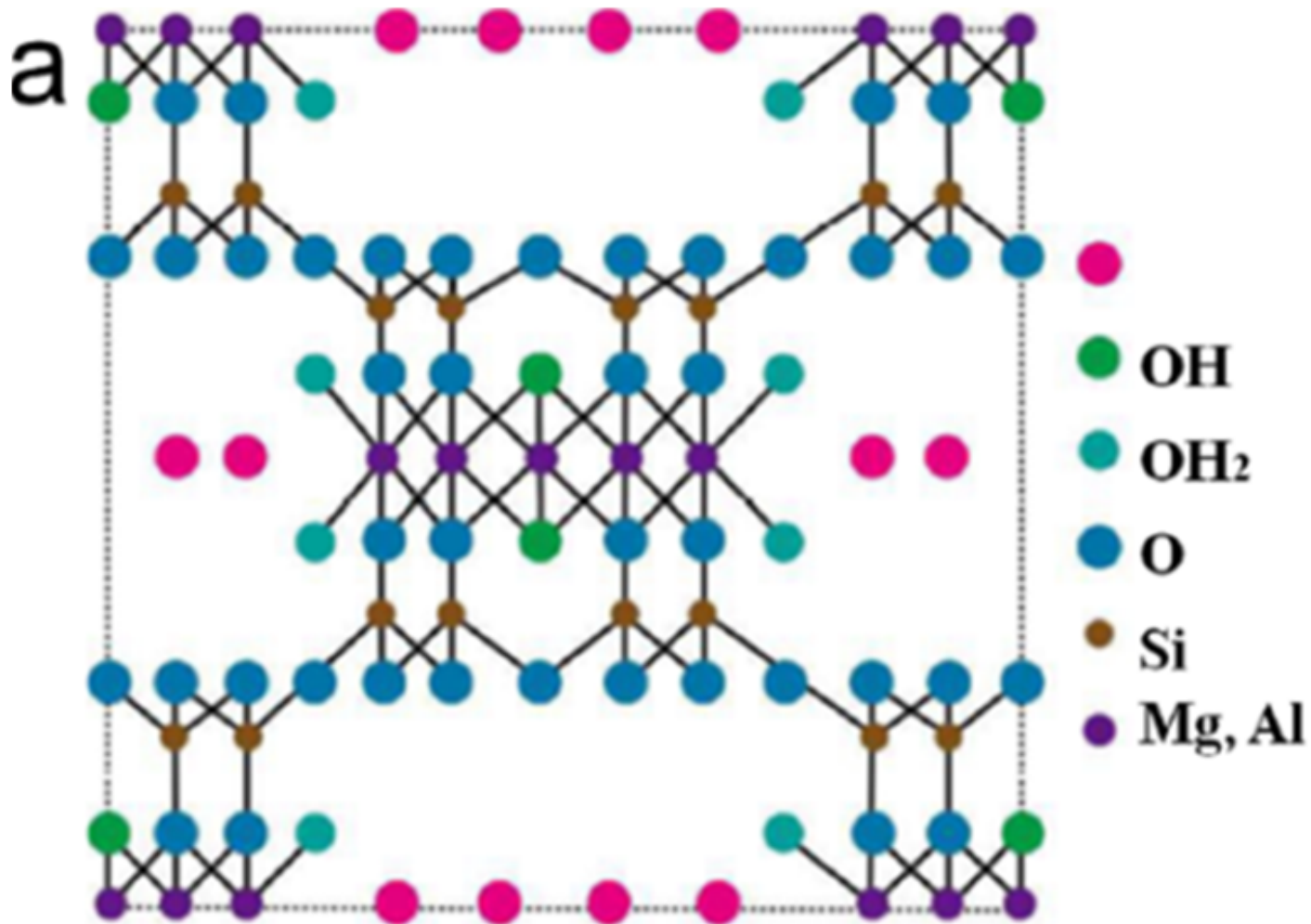
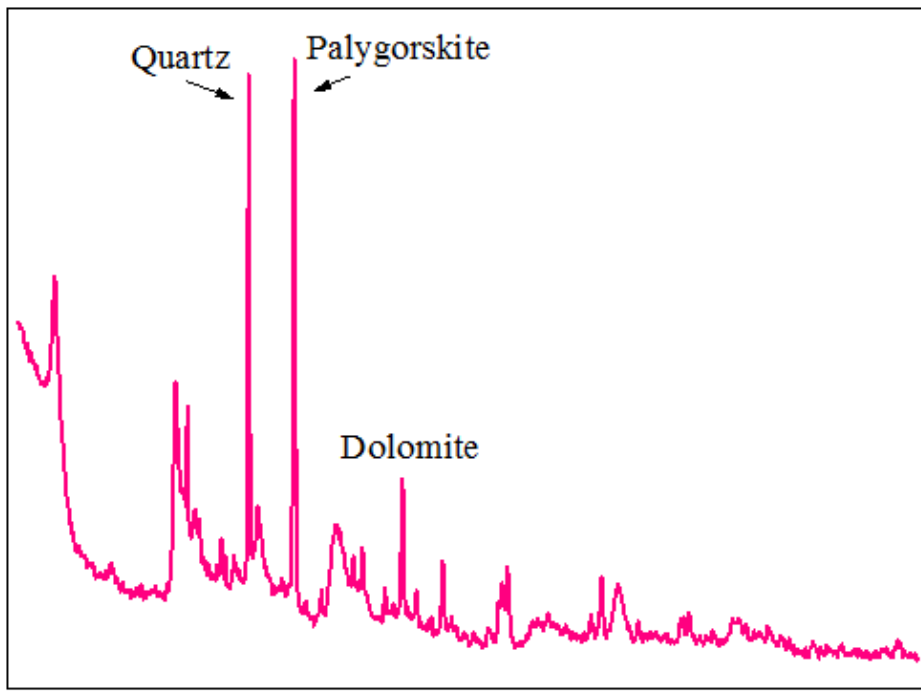


Figure 1

Attapulgite mineral structure



**Figure 2**

XRD pattern of attapulgite

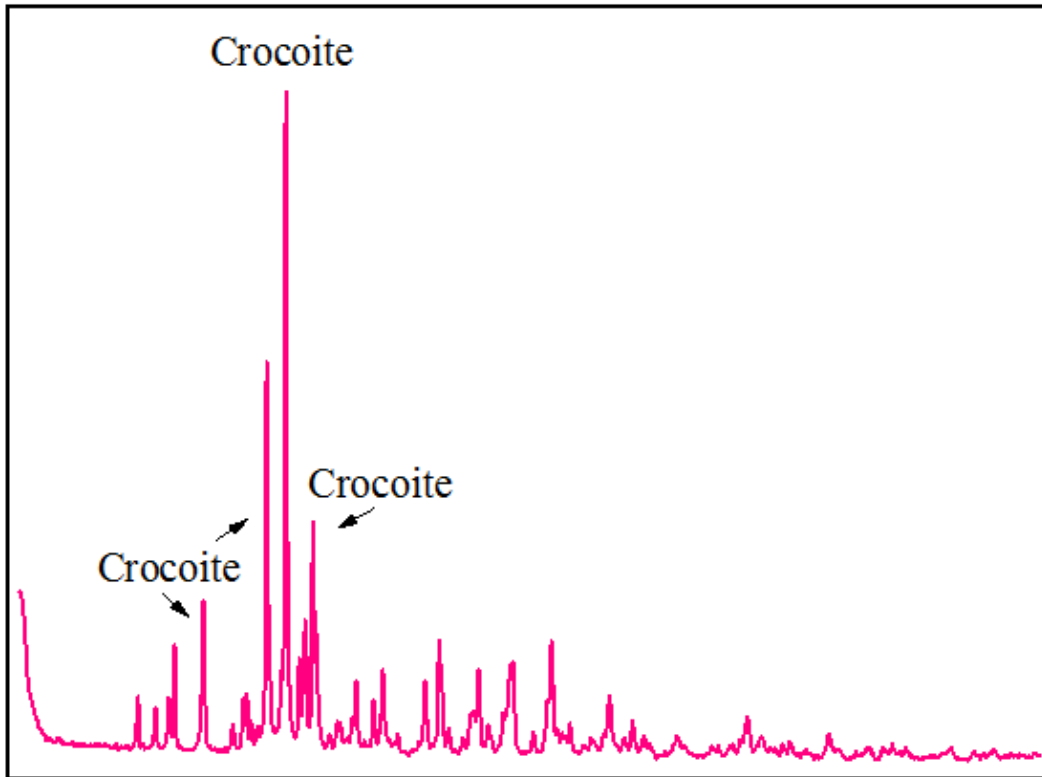


**Figure 3**

XRD pattern of the original sludge

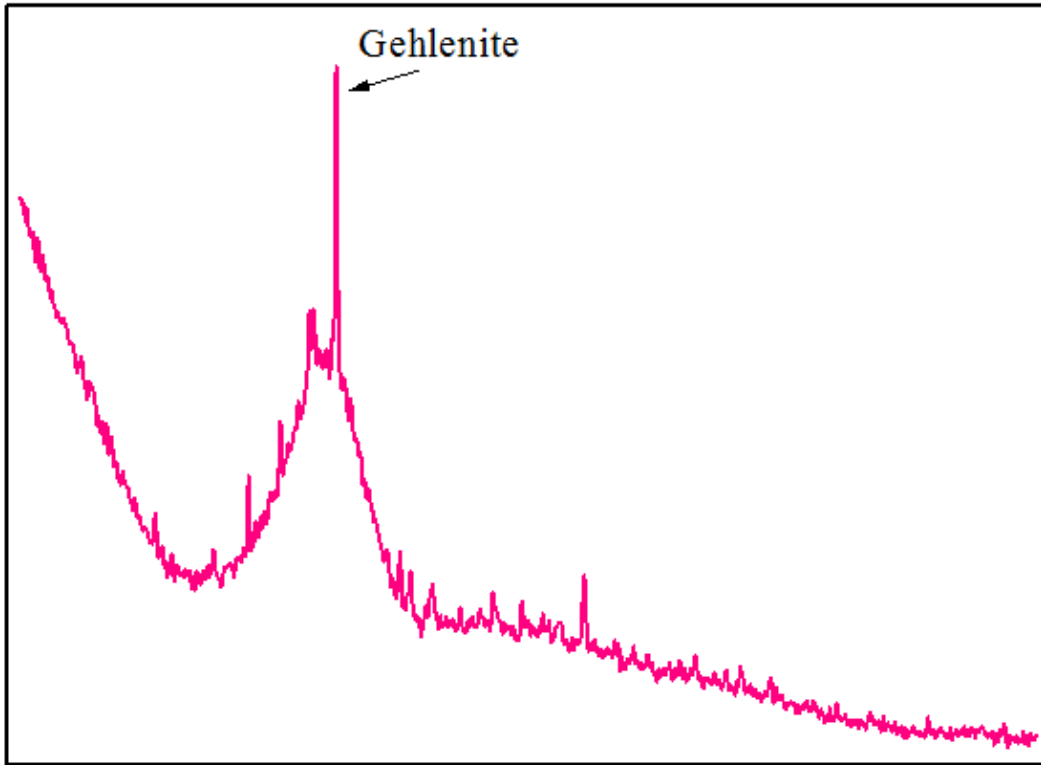


Figure 4

XRD pattern of slag

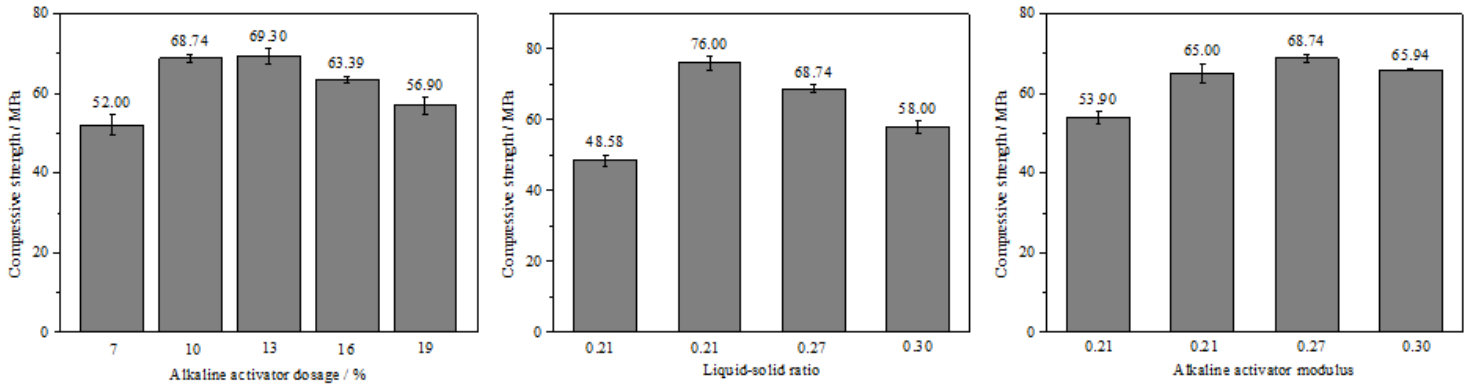


Figure 5

Single factor experiment results

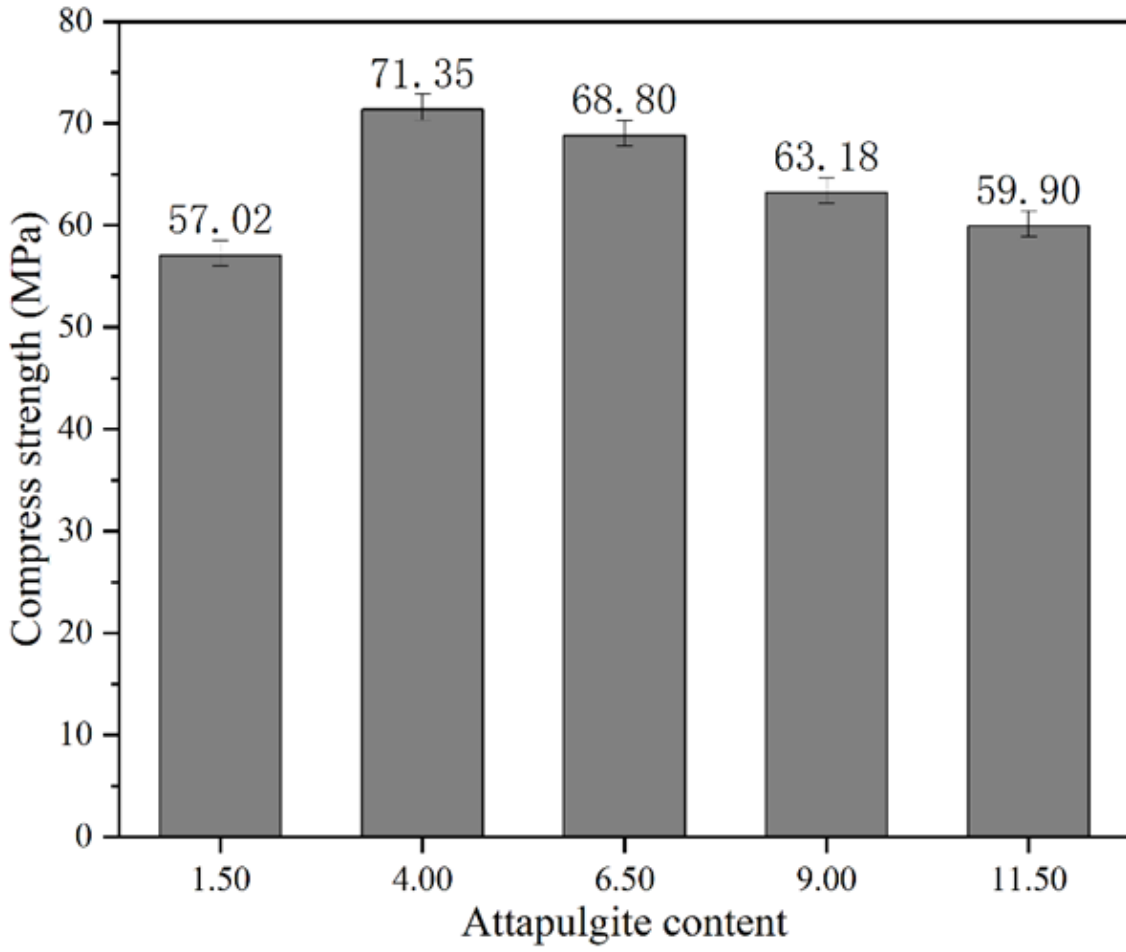


Figure 6

Influence of attapulgite content on compressive strength

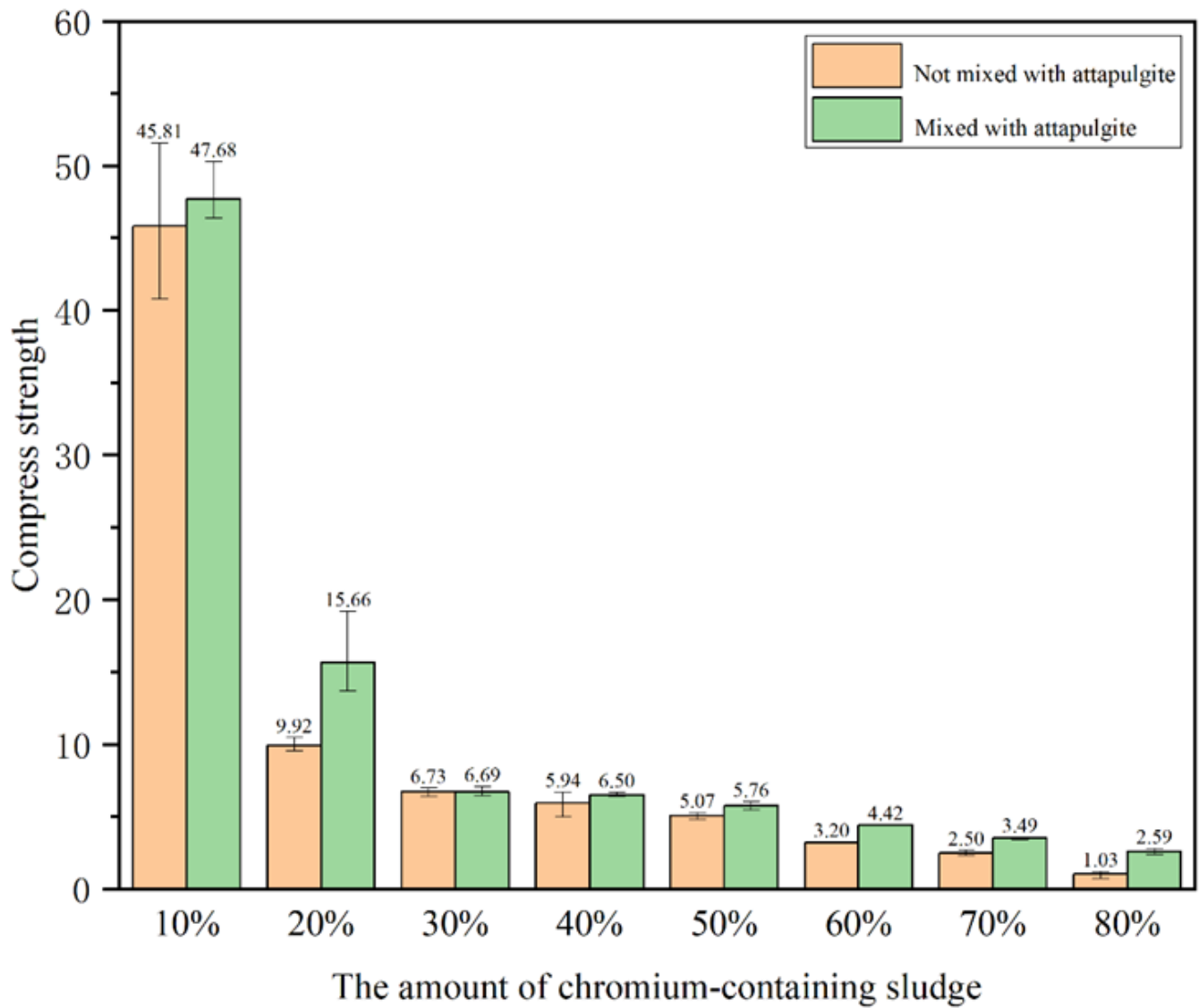


Figure 7

Comparison of compressive strength of solidified body before and after adding attapulgite

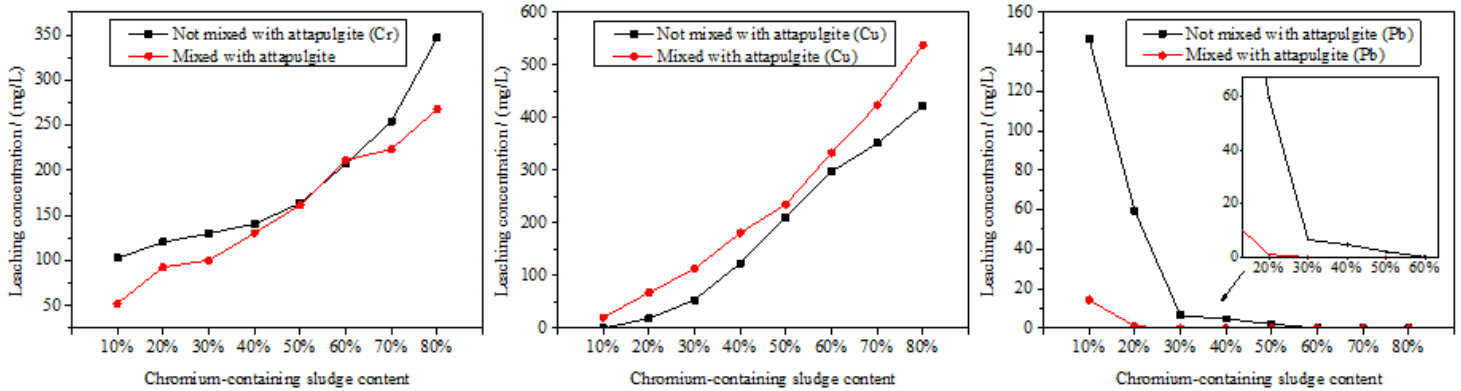


Figure 8

The leaching concentration of the solidified body

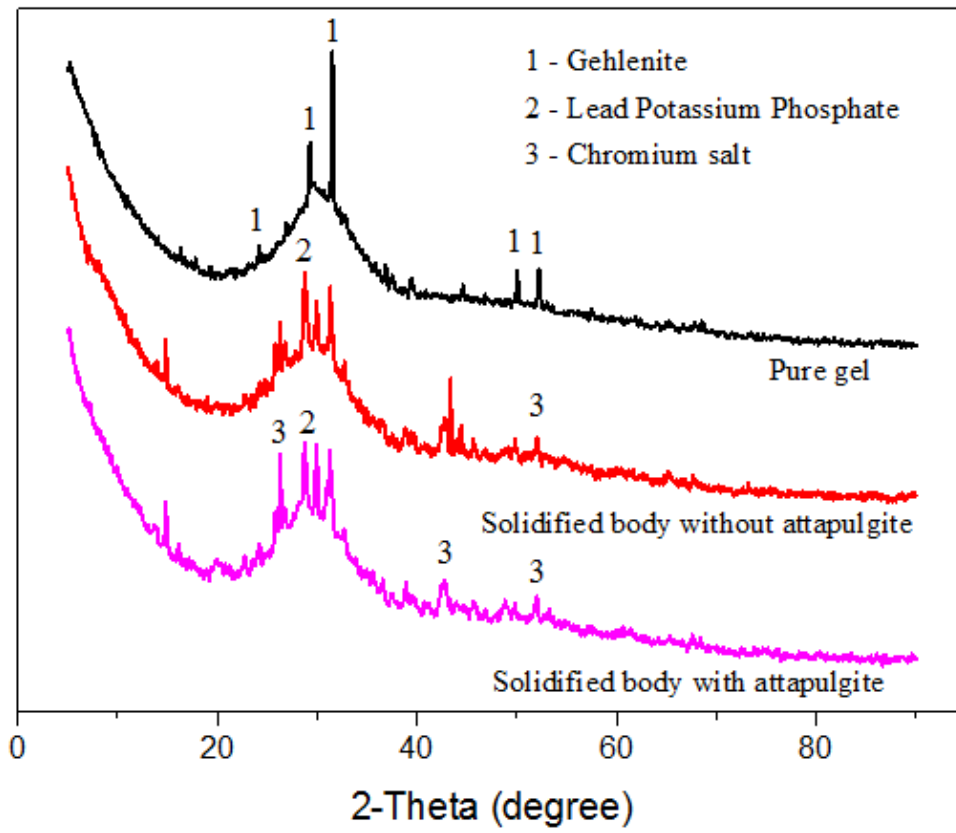


Figure 9

XRD pattern of each sample

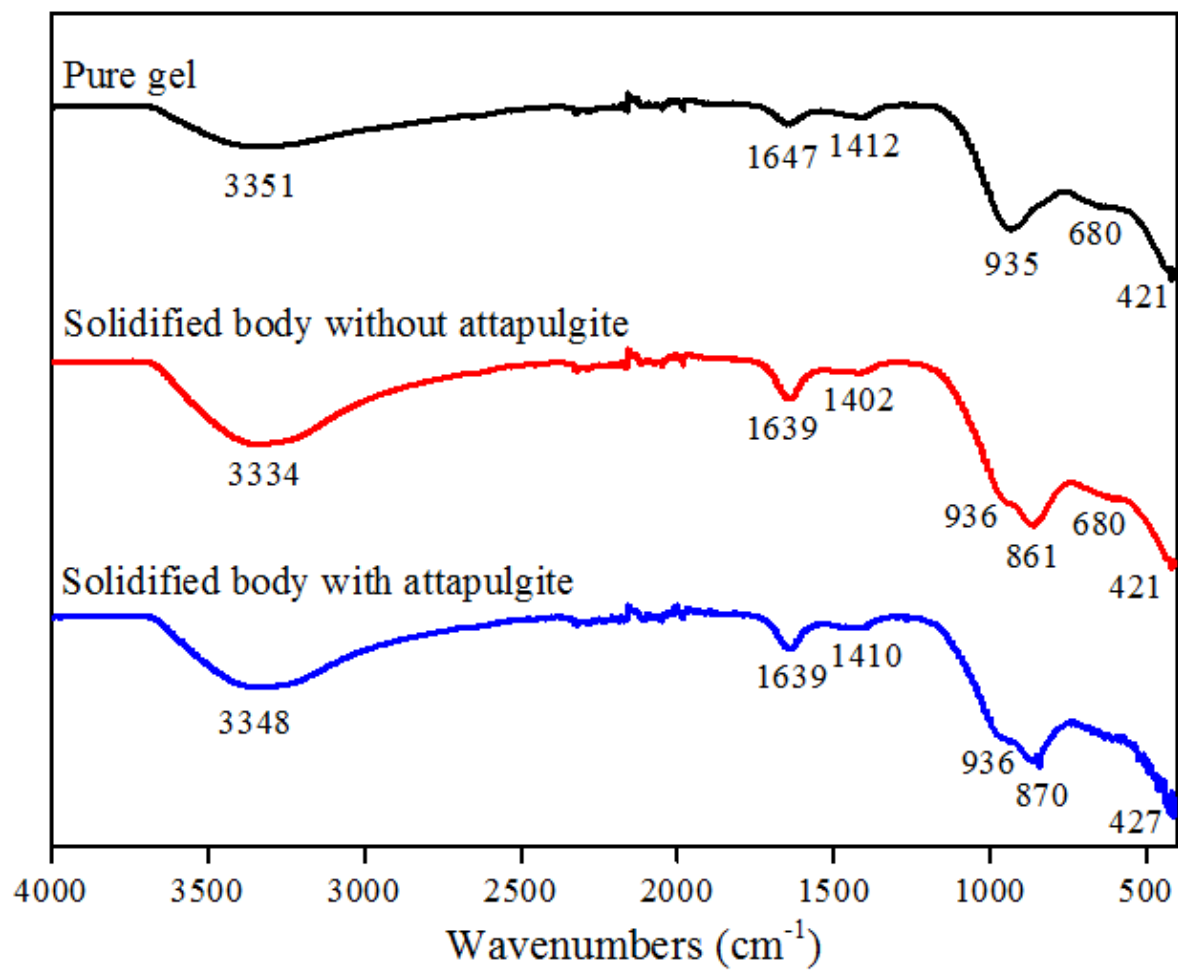


Figure 10

FTIR pattern of each sample